

CrossMark
click for updatesCite this: *J. Mater. Chem. A*, 2015, 3, 2181Received 29th October 2014
Accepted 25th November 2014

DOI: 10.1039/c4ta05810k

www.rsc.org/MaterialsA

From cotton to wearable pressure sensor†

Yuanqing Li,^{*a} Yarjan Abdul Samad^b and Kin Liao^{*ab}

In this work, carbon cottons (CC) with moderate electrical conductive (11 S m^{-1}) were prepared from cotton via a simple pyrolysis process. Flexible and electrical conductive CC/polydimethylsiloxane (PDMS) composites were fabricated by vacuum assisted infusion of PDMS resin into a CC scaffold. Based on the CC/PDMS composites prepared, a simple yet highly sensitive pressure sensor was developed, which shows a maximum sensitivity of 6.04 kPa^{-1} , a wide working pressure up to 700 kPa , a wide response frequency from 0.01 to 5 Hz , and durability over 1000 cycles. Based on our knowledge, the pressure sensitivity of the CC/PDMS sensor is only next to the record value in a pressure sensor (8.4 kPa^{-1}). By integrating the pressure sensor with a sport shoe and waist belt, we demonstrate that the real time sport performance and health condition could be monitored. Notably, the device fabrication process is simple and scalable with low-cost cotton as raw material. The CC/PDMS composites are believed to have promising potential applications in wearable electronic devices such as, human-machine interfacing devices, prosthetic skins, sport performance, and health monitoring.

Introduction

Flexible, sensitive, and low-cost pressure sensors are highly desirable in applications such as electronic skin, robot sensor, structural health monitoring, rehabilitation, personal health monitoring, and sport performance monitoring.^{1–3} However, conventional metal-foil and semiconductor slab pressure/strain sensors are limited to applications on both relatively stiff substrates and strains under 5% (beyond which the sensor fails mechanically) and therefore are unsuitable for flexible devices.^{4,5} Currently, various flexible pressure sensors that are based on capacitors,⁶ triboelectric nanogenerators,⁷ field-effect transistors,³ and piezoresistive materials have been successfully demonstrated.⁸ Among them, different nanomaterials, such as gold nanowire and nanoparticles,^{8–10} ZnO nanowire and nanorod,^{11–13} silver nanowire,¹ carbon nanofiber,¹⁴ carbon nanotube (CNT),^{4,15,16} and graphene^{2,17,18} are being exploited. However, these sensors either need elaborated nanostructural design that entail complicated and expensive fabrication procedures, or they are insensitive, unstable, and difficult to reproduce in low-pressure regimes, thus limiting their applications. Thus, it is still a great challenge to develop flexible and pressure-sensitive sensor with low-cost and large-area-compatible technology.

To date, there is a trend to produce carbon-based materials from biomass, as they are cheap, easy to acquire, sustainable, and environmentally friendly.¹⁹ Given their high porosity, flexibility, hydrophobicity, and electrical conductivity, porous carbon from biomass, such as bacterial cellulose, coconut, raw cotton, pomelo, water melon, winter melon and pumpkin, have shown a variety of potential applications in solar energy conversion and storage, super-capacitor, electromagnetic interference shielding, battery, and water treatment.^{19–25} Despite their superior mechanical and electrical properties, porous carbon from biomass have not yet been utilized in designing flexible sensors.

Herein, we demonstrate the fabrication of a simple-structured, low-cost flexible pressure sensor by vacuum infusion of

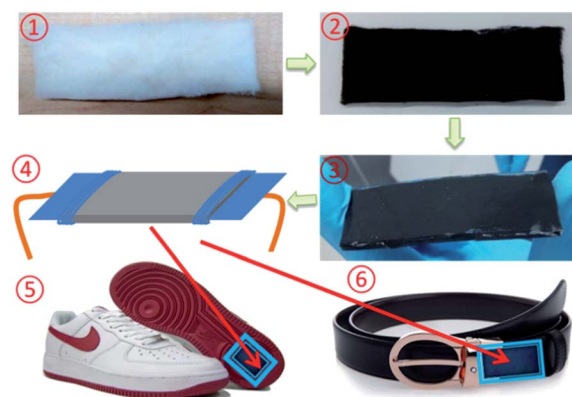


Fig. 1 Schematic of the fabrication of the wearable pressure sensor: (1) raw cotton, (2) carbon cotton, (3) CC/PDMS composite, (4) CC/PDMS pressure sensor, sensors integrated with sport shoe (5) and waist belt (6).

^aAerospace Engineering Department, Khalifa University of Science Technology & Research, Abu Dhabi 127788, United Arab Emirates. E-mail: yqli@mail.ipc.ac.cn; kin.liao@kustar.ac.ae; Fax: +971-2-4472442

^bMechanical Engineering Department, Khalifa University of Science Technology & Research, Abu Dhabi 127788, United Arab Emirates

† Electronic supplementary information (ESI) available: Electrical conductivities and mechanical properties, SEM images of raw cotton, RCR response of HCC/PDMS, the effect of thickness on the sensitivity of the sensor, response of CC/PDMS sensor with various maximum pressures. See DOI: 10.1039/c4ta05810k

polydimethylsiloxane (PDMS) into the carbon cotton (CC) made by pyrolysis cotton, illustrated in Fig. 1, which shows a maximum sensitivity of 6.04 kPa^{-1} with a wide working pressure range up to 700 kPa. Notably, CC, the key sensing element, can be easily fabricated in large scale by a simple synthetic method with cheap and ubiquitous cotton as the only raw material. Furthermore, by integrating the flexible pressure sensor with a sport shoe and waist belt, real time sport performance (such as working and running pace) and health condition (breathing) monitoring were demonstrated.

Experimental

Preparation of CC and CC/PDMS composites

Fluffy cotton used for quilt was purchased from ELS Textiles, UAE. Carbon cottons were obtained by simply placing sheet-shaped fluffy cotton in a tube furnace and pyrolyzed at $900 \text{ }^\circ\text{C}$ for 1 h in a N_2 atmosphere. The CC/PDMS composites were fabricated by a simple vacuum infusion process. First, a PDMS solution was prepared by homogeneously mixing the PDMS base agent and curing agent (Sylgard 184, Dow Corning) in the mass ratio of 10 : 1. Then CC sheets prepared were completely immersed in the PDMS solution. The mixture obtained was placed in a vacuum chamber for approximately 10 minutes to remove air bubbles. Finally, the CC/PDMS mixture was cured at $100 \text{ }^\circ\text{C}$ for 1 h. After the temperature of the CC/PDMS composite had cooled to room temperature, excessive PDMS that adhered on the surface of the composite was removed by a knife.

Characterizations

The morphology of raw cotton, CC, and CC/PDMS composites was imaged by a FEI Quanta FEG 250 scanning electron microscope (SEM). All optical pictures presented were taken by a digital camera (Canon IXUS 70). Electrical conductivity of the pure PDMS and CC/PDMS composite were measured at room temperature with a two-probe method using an insulation resistance meter (TH 2684A: 10 k Ω –100 T Ω) and a digital multimeter (ADM-930, 0.1 Ω –40 M Ω), respectively. The specimens used for conductivity measurement were silver-pasted to minimize the contact resistance between the specimens and the electrodes. The compression behavior of pure PDMS and CC/PDMS composites were investigated using a Microforce Tester (Instron 5948) at a loading rate of 1 mm min^{-1} , and the dimension of the tested samples was $8 \text{ mm} \times 8 \text{ mm} \times 4 \text{ mm}$. For electrical conductivity and compression test, more than 8 samples were tested, from which the average and standard deviation (SD) were calculated.

To study the pressure-sensing characteristic of the CC/PDMS composite, a simple pressure sensor was fabricated by fixing two aluminum foils on two sides of a CC/PDMS rectangular block ($15 \text{ mm} \times 50 \text{ mm} \times 4 \text{ mm}$) as electrodes. The fabricated CC/PDMS sensor was placed between the compression fixtures of the Microforce Tester, and each electrode of the sensor was connected with the electrode of an electrochemical workstation (Autolab 302N) by copper wires. When the compressive force/strain was applied to the sensor, the current changing under 1 V

from the sensor was recorded by the electrochemical workstation. Based on the current measured, the relative change of resistance (RCR, $\Delta R/R_0 = (R_p - R_0)/R_0$, where R_0 and R_p are the resistance without and with applied stress, respectively) were calculated. The pressure sensitivity, S , is defined as the slope of RCR–compression stress curve ($S = \delta(\Delta R/R_0)/\delta P$, where P denotes the applied stress). Similarly, the gauge factor, GF, is defined as the slope of RCR–strain curve ($\text{GF} = \delta(\Delta R/R_0)/\delta S$, where S denotes the applied strain).

To demonstrate the application of flexible sensor as a wearable device, a “smart” shoe was fabricated by integrating the sensor ($15 \text{ mm} \times 50 \text{ mm} \times 4 \text{ mm}$) on the heel of a sport shoe. The sport performances under walking, jogging, and running were monitored by the sensor. In addition, a “smart” waist belt was also fabricated by integrating the sensors ($10 \text{ mm} \times 40 \text{ mm} \times 1.5 \text{ mm}$) with the belt. Three breathing modes, normal breathing, breath holding, and deep breathing, were recorded by the sensor when a male adult breathed with the smart belt fastened to his waist.

Results and discussion

Raw cotton, a typical natural material with 90–95% cellulose, is a promising raw material to fabricate porous carbon.²³ The sponge like CC was prepared directly from the fluffy cotton by a simple pyrolysis process. As shown in Fig. 1, the black CC has maintained the original shape of raw cotton sheet, but the volume of the CC is only around 20% of that of the raw cotton. The porosity of CC, measured by the volume absorbance of the liquid, is close to 99%, rendering it an ultralow density of around 0.01 g cm^{-3} .

As shown in Fig. 2(A), CC has a porous structure and interconnected networks formed by carbon fibers. These fibers are very long with a diameter of 4–10 μm and an aspect ratio of 500–2000. Interestingly, as revealed by Fig. 2(B), these fibers have twists along the entire length of the fiber with a pitch length in the range of 10–20 μm . The twisted structure of carbon fiber originates from the naturally twisted structure of raw cotton fibers,²⁶ proved by the SEM images (Fig. S1 \dagger). Despite its ultralight weight and high porosity, as shown in Table S1 and Fig. S2, \dagger the CC from cotton exhibits an electrical conductivity of 11 S m^{-1} . The moderate electrical conductivity attributes to

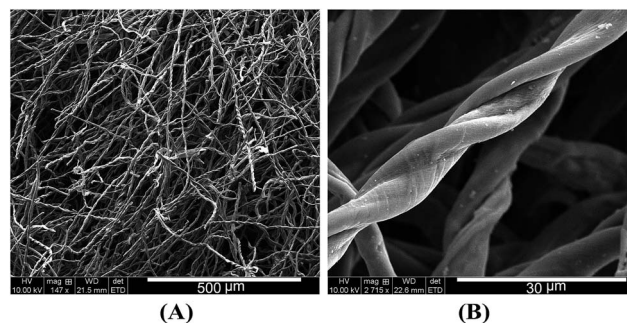


Fig. 2 (A) and (B) are SEM images of CC from cotton.

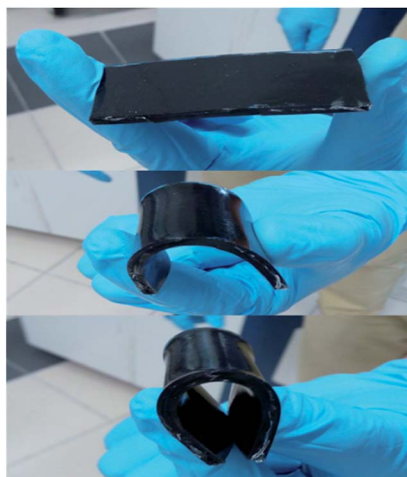


Fig. 3 Photographs show the flexibility of CC/PDMS composite.

the interconnected carbon fiber network, which provides a fast electron transport channel.

PDMS, a silicon-based elastomer with a repeating unit of $\text{SiO}(\text{CH}_3)_2$, is one of the most widely used polymer for fabricating flexible devices because of its high chemical stability and tunable mechanical properties. Taking the advantages of the high porosity of CC, CC/PDMS composites were fabricated by vacuum infusion of PDMS into the CC scaffold. After curing, the CC/PDMS composite maintains the same shape and size of the CC scaffold without visible void, indicating that the carbon fiber interconnections survived the infusion process. As revealed in Fig. 3, CC/PDMS composite displays excellent bendability.

Furthermore, the CC/PDMS composites can be easily compressed, and their original dimensions can be recovered immediately after releasing the load. Typical stress–strain curves during compression of pure PDMS and CC/PDMS composite are presented in Fig. 4. The compressive elastic modulus and stress at 20% strain of the CC/PDMS composite calculated are 4.35 MPa and 705 kPa, respectively. Compared with the elastic modulus and stress of pure PDMS (3.15 MPa and 558 kPa), a surge of 38% and 26%, respectively, are seen (Table S2†). The significant improvement in stiffness is mainly attributed to the fact that the compression elastic modulus of the carbon fiber is considerably higher than that of the PDMS matrix. From the rule of mixture, the elastic modulus of non-aligned fiber reinforced composite, E_C , is as follows:²⁷

$$E_C = (\eta_0 \eta_1 E_f - E_m) V_f + E_m \quad (1)$$

where V_f , E_f , and E_m are the volume fraction of the fiber, the elastic modulus of the fiber and matrix, respectively; η_0 is the orientation efficiency factor, for randomly oriented fiber, $\eta_0 = 1/5$; η_1 is the length efficiency factor and it approaches 1 for the filler with aspect ratio higher than 10. E_C and E_m measured are 4.35 and 3.15 MPa, respectively. Because the density of CC measured is 0.01 g cm^{-3} , suppose the real density of carbon fiber is 2 g cm^{-3} (typical value for carbon from biomass),²⁸ the volume fraction of fiber (V_f) in the composite is 0.5 percent by

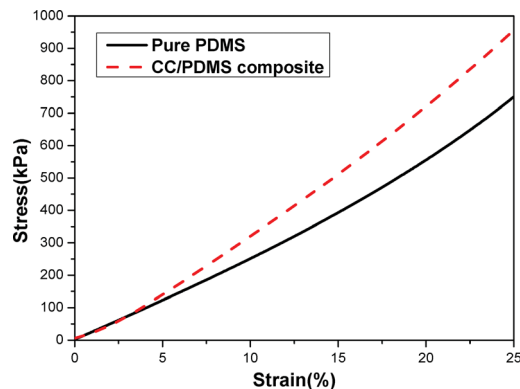


Fig. 4 Typical compression stress–strain curves of pure PDMS and CC/PDMS composite.

volume (vol%). The elastic modulus of carbon fiber estimated based on the rule of the mixture is 1.22 GPa.

Pure PDMS is a well-known insulator with electrical conductivity of $1.18 \times 10^{-11} \text{ S m}^{-1}$. However, the electrical conductivity of the CC/PDMS composite is 0.36 S m^{-1} , which is 10-order-of-magnitudes higher than that of pure PDMS. Considering the low CC loading ($\sim 0.5 \text{ vol}\%$), the electrical conductivity of CC/PDMS composites is considerably higher than those composites prepared from a conventional conductive filler, such as carbon black,²⁹ and this result is comparable to that prepared from a CNT and graphene based aerogel.³⁰ The interconnected network embedded in the polymer matrix by CC is the key factor for achieving the high electrical conductivity. Compared with CNT aerogel and graphene aerogel, the CC from cotton has the advantage of low cost, produced by a simple synthetic method, and easy scalable production.

With moderate electrical conductivity and high flexibility, the CC/PDMS composite could be a potential candidate for fabricating a flexible sensor. A prototype was fabricated by simply fixing two pieces of aluminium foil at each side of the CC/PDMS composite rectangular block as electrodes (Fig. 5(A)). Compared with most recently reported pressure sensors fabricated by either depositing or embedding sensing materials on the flexible substrates, in which the structure and performance of the sensors can be easily damaged even by mild touching,¹ sensors based on CC/PDMS composite can be easily fabricated and are considerably more reliable in performance. To investigate the response of the CC/PDMS sensor to pressure, a measuring system was designed by combining a Microforce Tester and an electrochemical workstation (Fig. 5(B)).

The current–voltage (I – V) characteristic of the CC/PDMS sensor under a pressure of 0 to 200 kPa was measured by applying a sweeping voltage from -3 to $+3 \text{ V}$. As shown in Fig. 6, all the I – V curves of the CC/PDMS sensor are linear, indicating an ohmic behavior and a constant resistance. It is seen that the slope of the I – V curves decreases with an increase in the applied pressure, indicating the corresponding rise in resistance under pressure. In addition, the change in resistance of the CC/PDMS sensor is revealed by the change in the brightness of a light-emitting diode (LED) integrated into the circuitry. As illustrated

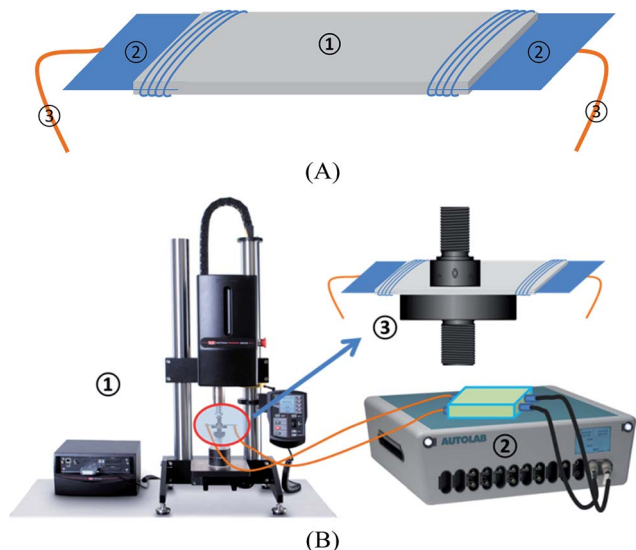


Fig. 5 (A) The schematic of CC/PDMS sensor: (1) CC/PDMS composite, (2) aluminium foil, (3) copper wire. (B) The schematic of CC/PDMS sensor performance measuring system: (1) Microforce tester – control the stress–strain applied, (2) electrochemical workstation – collect electrical signal, (3) sensor between compression fixtures.

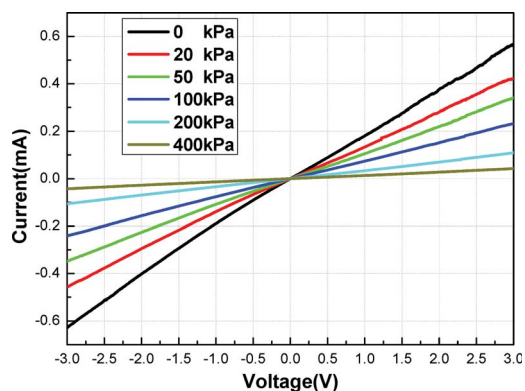


Fig. 6 Current–voltage curves of CC/PDMS sensor under different pressure.

in Fig. 7, the yellow LED light ceases when the pressure is applied and lights up again when the pressure is released. This change is reversible under cycling loading.

The relative change of resistance (RCR, $\Delta R/R_0$) is calculated on the basis of current value measured and is plotted as a function of applied compressive strain and stress (Fig. 8). As shown in the inset of Fig. 8, a linear relationship between RCR and stress is seen when the stress is less than 50 kPa, where the corresponding pressure sensitivity is around 2.2 kPa^{-1} . Further increase in stress results in an increase in the pressure sensitivity and it reaches 4.3 kPa^{-1} at 100 kPa. RCR increases continuously, with further increase of applied stress, and the sensor turns to an insulator at 700 kPa. Based on our knowledge, the pressure sensitivity of the CC/PDMS sensor is only next to the record value in a transistor pressure sensor (8.4 kPa^{-1}),³¹

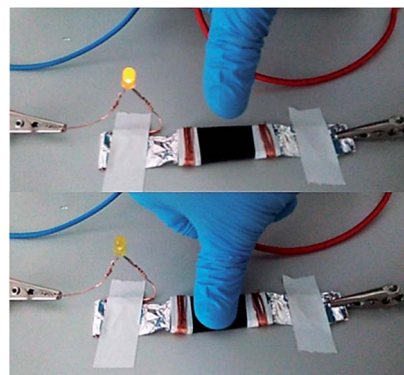


Fig. 7 The change in brightness of LED light by applying stress on the CC/PDMS sensor.

and it is higher than the typical sensitivity of 5×10^{-3} to 1.14 kPa^{-1} reported for other sensors.⁸ In addition, a linear relation between RCR and compression strain can be observed within a strain of 1.5%, and the gauge factor calculated is about 6.2, indicating CC/PDMS can also be used as a flexible strain sensor.

The pressure sensitivity of the CC/PDMS sensor can be adjusted by changing the electrical conductivity and thickness of the CC/PDMS composites. By compressing an as-prepared CC under 200 Pa for 24 h, a high density carbon cotton (HCC, around 0.02 g cm^{-3}) was obtained. The electrical conductivity of the HCC/PDMS composite prepared was significantly increased to 1.74 S m^{-1} . As shown in Fig. S3,[†] the pressure sensitivity of HCC/PDMS under low pressure (<30 kPa) and high pressure (150 kPa to 700 kPa) is only 0.45 kPa^{-1} and 0.027 kPa^{-1} , respectively. Compared with CC/PDMS, the pressure sensitivity of HCC/PDMS is considerably lower due to the denser CA fiber network constructed inside the PDMS matrix. In addition, the working stress for HCC/PDMS can be as high as 700 kPa, which is considerably higher than that of CC/PDMS (200 kPa). Moreover, the pressure sensitivity of CC/PDMS composite can also be adjusted by changing the thickness of the sensor. As shown in Fig. S4,[†] the pressure sensitivity of a 8 mm thick CC/PDMS

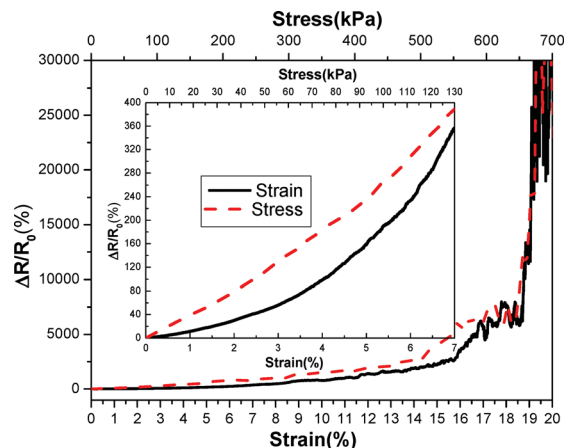


Fig. 8 Relative changing of resistance with applied compression strain–stress, and inset is the enlarged figure of initial part of curves.

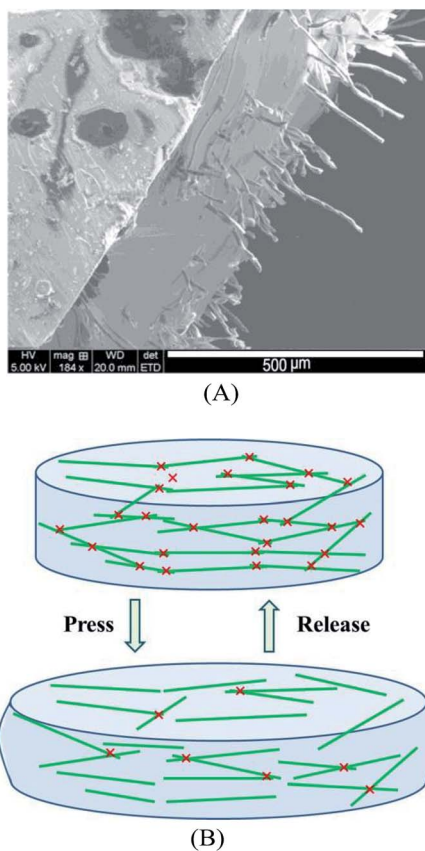


Fig. 9 (A) Fracture surface of the CC/PDMS composite; the sample was fractured by tension. (B) Schematic of the inner structure change in the CC/PDMS composite without and with applied stress: green lines represent the carbon fiber, and red crosses indicate the connection point of carbon fibers.

composite is only 0.33 kPa^{-1} . By reducing the thickness of the CA/PDMS composite to 1.5 mm, a very high pressure sensitivity (6.04 kPa^{-1}) is achieved. However, the linear relation between RCR and compression stress or strain of the sensor is lost when the thickness is further reduced, due to reduced connectivity between the carbon fiber inside the PDMS matrix. These results reveal that the thick CC/PDMS with high electrical conductivity is suitable for high pressure application with low sensitivity. Conversely, thin CC/PDMS with low electrical conductivity show better performance in low pressure applications with high sensitivity.

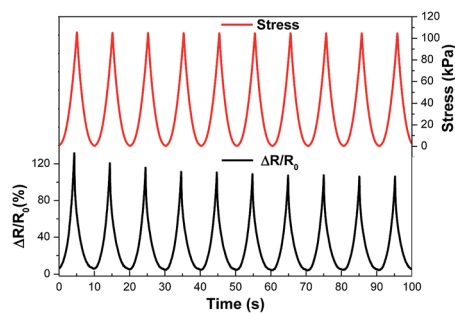
For a piezoresistive sensor, the variation of resistance is affected by the conducting paths and contact resistance between the nearby conductive fillers. For most of the pressure sensors based on conductive composites, upon compression, the connections between the neighboring conductive filler are enhanced, so that the composite becomes more conductive with lower resistance. However, the trend is reversed in our case. The difference in the mechanisms can be explained by the interaction between the PDMS matrix and carbon fibers. It is known that carbon fiber is considerably stiffer than the PDMS molecule. Under compression, carbon fibers behave like rigid rods, detach from and later slide in the surrounding PDMS matrix.

This assumption is verified by the tensile fracture surface of the CC/PDMS composite. As shown by Fig. 9(A), it is clear that the fracture surface is dominated by pullout of the carbon fiber from the PDMS matrix, indicating a weak CC-PDMS interface. Similar result has been observed in a strain sensor based on silver nanowire.¹ As illustrated in Fig. 9(B), the resistance of CC/PDMS composite is closely related to the amount of connection points formed by the carbon fiber within the PDMS matrix. Under compression, sliding of carbon fibers inside the PDMS matrix reduces the inter-fiber connection points, which induces a surge in the resistance. After releasing the applied load, ideally, all the carbon fibers should slide back to their initial position, and the resistance of the CC/PDMS is recovered.

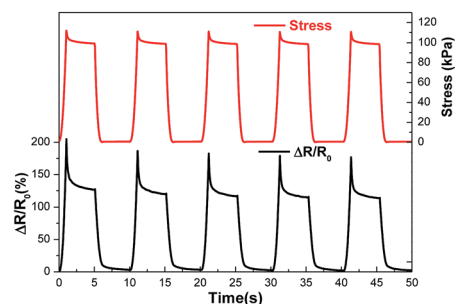
The response of CC/PDMS sensor to repeated compression-relaxation cycles was recorded and shown in Fig. 10. As shown in Fig. 10(A), there is an excellent agreement between the loading compression wave and the RCR response of the sensor without much drifting or hysteresis. Under different maximum loading (20 kPa to 200 kPa, Fig. S5[†]), the RCR response of the CC/PDMS is similar except the amplitude changes from 35% to 350%. Interestingly, RCR is influenced by the compression-relaxation wave form: it responds with a similar wave form of the applied compression-relaxation (Fig. 10(B)). In addition, the response of the CC/PDMS composite under repeated compression-relaxation cycles at a frequency range of 0.01 to 5 Hz is compared in Fig. 10(C). The frequency of the RCR response from the sensor agrees well with the frequency of applied compression, and a consistent behavior in the response of the sensor is observed from 0.01 to 5 Hz, which demonstrate the fast and stable response of the sensor. At the same time, it is evident that the amplitude of RCR under high frequency is considerably higher than that under low frequency, which attributes to the fact that stress applied on the sensor with fixed strain under high frequency is considerably higher than that under low frequency. The durability of the CC/PDMS pressure sensor was tested under a pressure of 100 kPa at a frequency of 1 Hz. As shown in Fig. 10(D), the response and RCR amplitude of the CC/PDMS sensor is maintained after 1000 compression-relaxation cycles.

To demonstrate the feasibility of the CC/PDMS sensor as a wearable device, a "smart" sport shoe integrated with the CC/PDMS sensor was fabricated (Fig. 1). The real time sport performance, such as walking, jogging, and running, can be well monitored. As shown in Fig. 11(A), it is clear that the pace and shoes/ground contact modes varies under different modes of movement. The pace calculated from walking, jogging, and running is 36, 63, and 72 steps per minutes, respectively. For walking and jogging, it is found that the shoes in air time is quite similar with an average time around 0.7 s, whereas the main difference is that jogging has a considerably shorter shoes/ground contact time (0.23 s) than that of walking (0.97 s). For running, the reduced shoe-in-air time and shoes/ground contact time both contribute to the improvement of the running pace. In addition, the stress applied on the shoe can also be analyzed based on the response of the RCR amplitude.

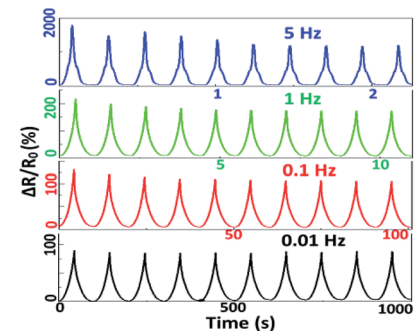
Real time breathing detection was carried out by integrating the CC/PDMS sensor with a waist belt (Fig. 1). Three breathing



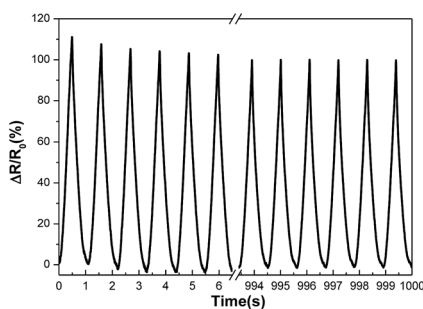
(A)



(B)

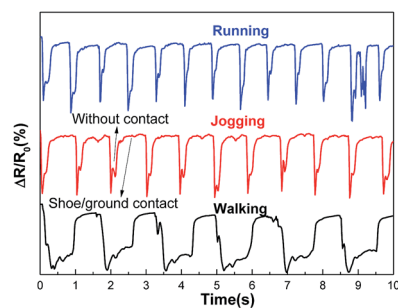


(C)

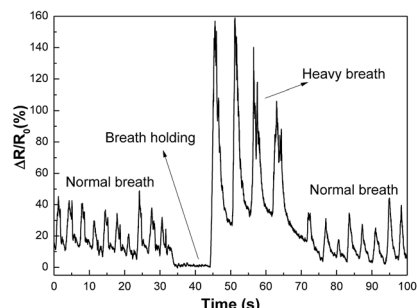


(D)

Fig. 10 Response of the CC/PDMS sensor under repeated compression–relaxation cycles (A) and compression–hold–relaxation–hold cycles (B), in the range of 0–100 kPa at 0.1 Hz. (C) Response of the CC/PDMS sensor at frequencies from 0.01 Hz to 5 Hz. (D) Reliability test of the CC/PDMS sensor under repeated compression–relaxation cycles in the range of 0–100 kPa.



(A)



(B)

Fig. 11 Real-time sport performance (A) and breathing (B) monitoring by CC/PDMS sensor.

patterns, namely, normal breathing, breath holding, and deep breathing, can be easily distinguished from the RCR response curve (Fig. 11(B)). It is clear that the RCR amplitude under deep breathing is considerably larger than that from normal breathing, whereas it is a constant under breath holding. Apart from tracing the amplitude of breathing, the breathing rate is easily counted to be approximately 20 and 10 times per minute for normal breathing and deep breathing, respectively. These results demonstrate that the CC/PDMS composite is suitable to fabricate a wearable device to monitor human health and sport performance.

Conclusions

In this work, low density carbon cottons with moderate electrical conductive (11 S m^{-1}) were prepared from cotton *via* a simple pyrolysis process. Flexible and electrical conductive CC/PDMS composites were fabricated by vacuum assisted infusion of PDMS resin into a CC scaffold. Based on the CC/PDMS composites prepared, a simple yet highly sensitive pressure sensor was developed, which shows a maximum sensitivity of 6.04 kPa^{-1} , a wide working pressure up to 700 kPa, a wide response frequency from 0.01 to 5 Hz, and a high durability over 1000 cycles. By integrating the pressure sensor with a sport shoe and waist belt, we demonstrate that the real time sport performance and health condition could be monitored. Notably, the device fabrication process is simple and scalable with low-cost cotton as raw materials. The CC/PDMS composites are believed

to have promising potential applications in wearable electronic devices such as, human-machine interfacing devices, prosthetic skins, sport performance, and health monitoring.

Acknowledgements

The authors are grateful to the financial support by the Khalifa University Internal Research Funds (no. 210008 and no. 210038).

Notes and references

- 1 M. Amjadi, A. Pichitpajongkit, S. Lee, S. Ryu and I. Park, *ACS Nano*, 2014, **8**, 5154.
- 2 H.-B. Yao, J. Ge, C.-F. Wang, X. Wang, W. Hu, Z.-J. Zheng, Y. Ni and S.-H. Yu, *Adv. Mater.*, 2013, **25**, 6692.
- 3 T. Tran Quang, T. Nguyen Thanh, D. Kim, M. Jang, O. J. Yoon and N.-E. Lee, *Adv. Funct. Mater.*, 2014, **24**, 117.
- 4 D. J. Cohen, D. Mitra, K. Peterson and M. M. Maharbiz, *Nano Lett.*, 2012, **12**, 1821.
- 5 A. Bessonov, M. Kirikova, S. Haque, I. Gartsev and M. J. A. Bailey, *Sens. Actuators, A*, 2014, **206**, 75.
- 6 S. C. B. Mannsfeld, B. C. K. Tee, R. M. Stoltenberg, C. V. H. H. Chen, S. Barman, B. V. O. Muir, A. N. Sokolov, C. Reese and Z. Bao, *Nat. Mater.*, 2010, **9**, 859.
- 7 F.-R. Fan, L. Lin, G. Zhu, W. Wu, R. Zhang and Z. L. Wang, *Nano Lett.*, 2012, **12**, 3109.
- 8 S. Gong, W. Schwalb, Y. W. Wang, Y. Chen, Y. Tang, J. Si, B. Shirinzadeh and W. L. Cheng, *Nat. Commun.*, 2014, **5**, 3132.
- 9 C. Farcau, N. M. Sangeetha, H. Moreira, B. Viallet, J. Grisolia, D. Ciuculescu-Pradines and L. Ressler, *ACS Nano*, 2011, **5**, 7137.
- 10 V. Maheshwari and R. F. Saraf, *Science*, 2006, **312**, 1501.
- 11 W. G. Zhang, R. Zhu, V. Nguyen and R. S. Yang, *Sens. Actuators, A*, 2014, **205**, 164.
- 12 H. Gullapalli, V. S. M. Vemuru, A. Kumar, A. Botello-Mendez, R. Vajtai, M. Terrones, S. Nagarajaiah and P. M. Ajayan, *Small*, 2010, **6**, 1641.
- 13 X. Xiao, L. Yuan, J. Zhong, T. Ding, Y. Liu, Z. Cai, Y. Rong, H. Han, J. Zhou and Z. L. Wang, *Adv. Mater.*, 2011, **23**, 5440.
- 14 H. A. K. Toprakci, S. K. Kalanadhabhatla, R. J. Spontak and T. K. Ghosh, *Adv. Funct. Mater.*, 2013, **23**, 5536.
- 15 X. Gui, A. Cao, J. Wei, H. Li, Y. Jia, Z. Li, L. Fan, K. Wang, H. Zhu and D. Wu, *ACS Nano*, 2010, **4**, 2320.
- 16 S. Li, J. G. Park, S. Wang, R. Liang, C. Zhang and B. Wang, *Carbon*, 2014, **73**, 303.
- 17 Y. Wang, L. Wang, T. T. Yang, X. Li, X. B. Zang, M. Zhu, K. L. Wang, D. H. Wu and H. W. Zhu, *Adv. Funct. Mater.*, 2014, **24**, 4666.
- 18 S.-H. Bae, Y. Lee, B. K. Sharma, H.-J. Lee, J.-H. Kim and J.-H. Ahn, *Carbon*, 2013, **51**, 236.
- 19 Y. Q. Li, Y. A. Samad, K. Polychronopoulou, S. M. Alhassan and K. Liao, *ACS Sustainable Chem. Eng.*, 2014, **2**, 1492.
- 20 Y. Q. Li, Y. A. Samad, K. Polychronopoulou, S. M. Alhassan and K. Liao, *J. Mater. Chem. A*, 2014, **2**, 7759.
- 21 J. Zhang, J. Y. Xiang, Z. M. Dong, Y. Liu, Y. S. Wu, C. M. Xu and G. H. Du, *Electrochim. Acta*, 2014, **116**, 146.
- 22 X. L. Wu, T. Wen, H. L. Guo, S. B. Yang, X. K. Wang and A. W. Xu, *ACS Nano*, 2013, **7**, 3589.
- 23 Z. Y. Wu, C. Li, H. W. Liang, J. F. Chen and S. H. Yu, *Angew. Chem., Int. Ed.*, 2013, **52**, 2925.
- 24 Q. L. Liu, J. J. Gu, W. Zhang, Y. Miyamoto, Z. X. Chen and D. Zhang, *J. Mater. Chem.*, 2012, **22**, 21183.
- 25 H. C. Bi, Z. Y. Yin, X. H. Cao, X. Xie, C. L. Tan, X. Huang, B. Chen, F. T. Chen, Q. L. Yang, X. Y. Bu, X. H. Lu, L. T. Sun and H. Zhang, *Adv. Mater.*, 2013, **25**, 5916.
- 26 S. Gordon and Y. L. Hsieh, *Cotton Science and Technology*, Woodhead Publishing, Sawston, Cambridge, UK, 2007.
- 27 Y. Q. Li, T. Y. Yang, T. Yu, L. X. Zheng and K. Liao, *J. Mater. Chem.*, 2011, **21**, 10844.
- 28 A. V. Kurdyumov, V. F. Britun, O. Y. Khyzhun, Y. V. Zaulychnyy, V. L. Bekenev, V. O. Dymarchuk and A. I. Danilenko, *Diamond Relat. Mater.*, 2011, **20**, 974.
- 29 W. Yi, Y. Wang, G. Wang and X. Tao, *Polym. Test.*, 2012, **31**, 677.
- 30 Y. Li, Y. A. Samad, K. Polychronopoulou, S. M. Alhassan and K. Liao, *Sci. Rep.*, 2014, **4**, 4652.
- 31 G. Schwartz, B. C. K. Tee, J. Mei, A. L. Appleton, D. H. Kim, H. Wang and Z. Bao, *Nat. Commun.*, 2013, **4**, 1859.